Van der Ploeg, L. H. T., Groffen, J., & Flavell, R. A. (1980) *Nucleic Acids Res. 8*, 4563–4574.
Wang, A. H.-J., Quigley, G. J., Kolpak, F. J., Crawford, J. L., Van Boom, J. H., Van der Marel, G. A., & Rich, A. (1979) *Nature (London) 282*, 680–686.
Wang, A. H.-J., Quigley, G. J., Kolpak, F. J., Van der Marel, G., Van Boom, J. H., & Rich, A. (1981) *Science (Washington, D.C.) 211*, 171–176.

Sequential Resonance Assignments in ^{1}H NMR Spectra of Oligonucleotides by Two-Dimensional NMR Spectroscopy†

R. M. Scheek, R. Boelens, N. Russo,‡ J. H. van Boom,§ and R. Kaptein*

ABSTRACT: A sequential assignment procedure is outlined, based on two-dimensional NOE (NOESY) and two-dimensional *J*-correlated spectroscopy (COSY), for assigning the nonexchangeable proton resonances in NMR spectra of oligonucleotides. As presented here the method is generally applicable to right-handed helical oligonucleotides of intermediate size. We applied it to a *lac* operator DNA fragment consisting of d(TGAGCGG) and d(CCGCTCA) and obtained complete assignments for the adenine H8, guanine H8, cytosine H6 and H5, thymine H6 and 5-methyl, and the deoxyribose H1′, H2′, H2″, H3′, and H4′ resonances, as well as some H5′, H5″ (pairwise) assignments. These assignments are required for the analysis of two-dimensional NOE and *J*-coupling data in terms of the solution structure of oligonucleotides.

Although potentially NMR gives the most detailed information on the structure of biomolecules in solution, the analysis of NMR spectra has been hampered by the difficulty of obtaining resonance assignments. For proteins this situation has changed recently as two-dimensional NMR techniques have made it possible to translate the known primary structure of the molecule into resonance assignments via so-called sequential-assignment methods (Wüthrich et al., 1982). The same techniques can be used to yield information about secondary and tertiary protein structure, as demonstrated recently for the *lac* repressor headpiece (Zuiderweg et al., 1983).

Feigon et al. (1982) were the first to use 2-D NMR[1] in the study of a double-stranded oligonucleotide and observed some interesting intra- and internucleotide NOE's. In this paper we wish to present a systematic method based on 2-D NMR for assigning resonances of the nonexchangeable protons in nucleic acids.[2] Thus far most of the attention of NMR spectroscopists has been directed to the low-field region of nucleic acid spectra, where the imino protons resonate that take part in the hydrogen bonds of Watson–Crick base pairs. Assignment strategies for these protons have been based upon chemical-shift calculations (Bell et al., 1983) or the study of melting behavior (Zuiderweg et al., 1981) and, more recently, on the nuclear Overhauser effect (NOE) (Redfield et al., 1981; Patel et al., 1982), which is observable between imino protons in neighboring base pairs. However, the cross-relaxation network formed by these protons does not extend to the exterior regions of the molecule, and of the nonexchangeable protons only the adenine H2 protons can be assigned via this approach.

The sequential assignment procedure presented here for the remaining, nonexchangeable protons in nucleic acids can be applied to right-handed helical oligonucleotides. Its application will be demonstrated for a seven base pair DNA duplex consisting of the two complementary heptanucleotides d(TGAGCGG) and d(CCGCTCA), where it yields the assignments of all purine H8, pyrimidine H6, cytosine H5, thymine CH_3, and deoxyribose H1′, H2′, H2″, H3′, and H4′ resonances, as well as some of the H5′ and H5″ resonances. These assignments may form the basis of a more detailed study of the structure of the DNA duplex in solution.

Materials and Methods

^{1}H NMR spectra were recorded at 360 MHz on a Bruker HX360 and at 500 MHz on a Bruker WM500 spectrometer, equipped with Aspect 2000 computers.

Two-dimensional NOE spectra were recorded by using the pulse sequence $(\pi/2\text{–}t_1\text{–}\pi/2\text{–}\tau_m\text{–}\pi/2\text{–Acq})_n$, described by Macura & Ernst (1980). Phase cycling was performed according to States et al. (1982); the carrier position was at the low-field side of the spectrum, so that only real t_1 data had to be collected. A total of 512 FID's, 2048 data points each, was recorded for each spectrum. These were transferred to a Cyber 170-760 computer via magnetic tape for processing. Before Fourier transformation the FID's were weighed with a 45–60°-shifted sine-bell function and zero filled to 4096 points. After phase correction the real matrix was transposed, and the interferograms were weighed with a similar sine bell, zero-filled to 2048 points, and Fourier transformed. Phase correction and symmetrization then yield a 1024 × 1024 spectrum in pure absorption phase.

COSY spectra were recorded with the $(\pi/2\text{–}t_1\text{–}\pi/2\text{–Acq})_n$ sequence described by Aue et al. (1976). A total of 512 FID's was recorded, each of 2048 points, with the carrier frequency outside the spectrum. Both FID's and interferograms were weighed with an unshifted sine-bell function before zero filling and Fourier transformation. Spectra are presented in the absolute-value mode and symmetrized.

† From the Department of Physical Chemistry, University of Groningen, Groningen, The Netherlands. *Received July 28, 1983.* This work was supported by the Netherlands Foundation for Chemical Research (SON) with financial aid from the Netherlands Organization for the Advancement of Pure Research (ZWO).

‡ Present address: Dipartimento di Chimica, Universita degli Studi della Calabria, Arcavacata di Rende, Italia.
§ Present address: Department of Organic Chemistry, University of Leiden, Leiden, The Netherlands.

[1] Abbreviations: FID, free induction decay; 2-D, two-dimensional; NMR, nuclear magnetic resonance; NOE, nuclear Overhauser effect; COSY, two-dimensional *J*-correlated spectroscopy; ppm, parts per million; DSS, 4,4-dimethyl-4-silapentane-1-sulfonate; bp, base pair; A, adenine, T, thymine; C, cytosine; G, guanine; B, purine H8 (AH8 or GH8) or pyrimidine H6 (CH6 or TH6).

[2] For a preliminary report of this work, see Scheek et al. (1983).

0006-2960/84/0423-1371$01.50/0

Table I: Proton-Proton Distances[a] (nm) in B-DNA

type of contact	B-B	B-CH5	B-TCH_3	B-H1′	B-H2′	B-H2″	CH5-H2′	CH5-H2″	TCH_3-H2′	TCH_3-H2″
intranucleotide (*i*,*i*)		0.24	0.28	0.38	0.21	0.36	0.42	0.55	0.45	>0.6
to 3′ neighbor (*i*,*i* + 1)	0.50	0.38	0.32	>0.6	>0.6	>0.6	>0.6	>0.6	>0.6	>0.6
to 5′ neighbor (*i*,*i* − 1)	0.50	>0.6	>0.6	0.28	0.37	0.23	0.32	0.28	0.25	0.22

[a] Proton coordinates were calculated on the basis of the X-ray coordinates of B-DNA (Arnott & Hukins, 1972) and a C-H bond length of 0.109 nm. For distances involving TCH_3 protons an apparent distance was calculated from the value of r_{ij}^{-6}, averaged over six different methyl-proton positions, according to the formula $r_{ij}^{app} = (1/6\Sigma_{i=1}^{6} r_{ij}^{-6})^{-1/6}$. Distances for all combinations of nucleotides fall within 0.015 nm from the average given in the table.

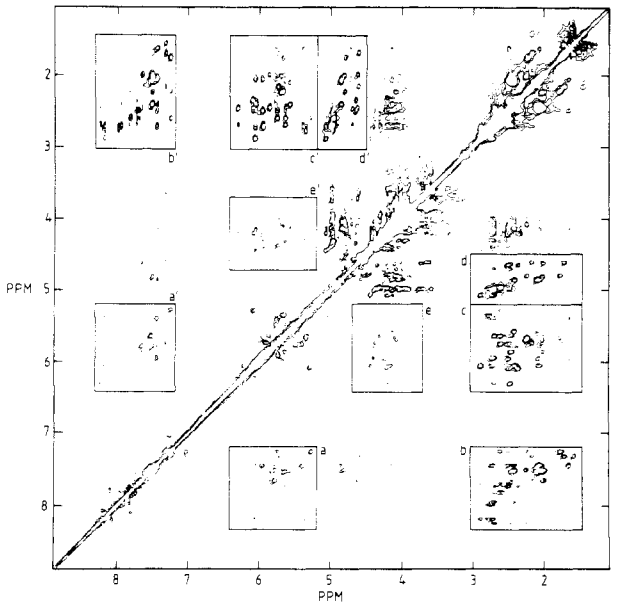

FIGURE 1: 500-MHz 2-D NOE spectrum of an equimolar mixture of d(TGAGCGG) and d(CCGCTCA). The spectrum is a sum of three 2-D NOE spectra with mixing times τ_m = 80, 120, and 160 ms that were recorded to obtain NOE buildup curves as shown in Figure 9.

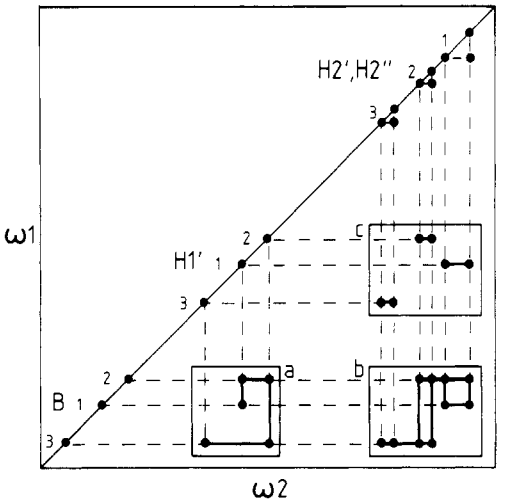

FIGURE 2: Schematic 2-D NOE spectrum of a trinucleotide in a right-handed helix conformation. Numbering of nucleotides starts at the 5′ end. Regions a, b, and c correspond to the regions in Figure 1 indicated with these symbols. The dipolar-coupling patterns involving the B, H1′, H2′, and H2″ resonances are indicated with drawn lines in regions a and b; the three H1′–H2′, H2″(*i*,*i*) connectivity pairs are shown in region c. See text for a detailed explanation of the sequential assignment procedure for these resonances.

The heptanucleotides were synthesized as described elsewhere (van Boom et al., 1976; De Rooij et al., 1979). Solutions were 5 mM DNA in 50 mM KP_i, 0.2 M NaCl, and 0.02% NaN_3, pH 6.5 (meter reading) in ^2H_2O, 28 °C.

Results

Strategy for Sequential Assignments in ^1H NMR Spectra of Oligonucleotides. Figure 1 shows a 2-D NOE spectrum of the duplex formed by d(TGAGCGG) and d(CCGCTCA). As described in detail by Macura & Ernst (1980) cross peaks in a 2-D NOE spectrum correlate the chemical shifts of nuclei between which magnetization is transferred during the mixing time by incoherent processes (in our case cross relaxation) and via zero-quantum coherence. Thus, a cross peak linking two diagonal resonances is diagnostic for the proximity (less than ~0.4 nm) of the protons involved. We use the following terminology to indicate DNA resonances and cross peaks: numbering of nucleotides starts at the 5′ end. Purine H8 and pyrimidine H6 protons, which occupy very similar positions in a regular helix, are treated as a group and named B (base) protons. A cross peak B–H2′(*i*,*j*) connects the purine H8 or pyrimidine H6 resonance of nucleotide *i* in a given strand with the H2′ resonance of nucleotide *j* at frequencies $(\omega_1, \omega_2) = (\Omega_{B(i)}, \Omega_{H2'(j)})$.

Direct "contacts" between B resonances in adjacent nucleotides are normally too weak to be useful for a sequential-assignment procedure. However, the ribose H1′, H2′, and H2″ protons of a certain nucleotide are close enough not only to the B proton in the same nucleotide but also to the B proton of the 3′-neighboring one to generate NOE cross peaks (regions a and b in Figure 1). Thus, a cross-relaxation network involving these protons extends throughout each strand of the DNA duplex. In addition, when a pyrimidine occurs in the strand, the cytosine H5 or thymine CH_3 resonances show strong intranucleotide cross peaks with B resonances but also internucleotide cross peaks with B, H2′, and H2″ resonances of the 5′-neighboring nucleotide. Table I presents the relevant proton–proton distances, calculated on the basis of a regular B-DNA conformation. The assignment procedure then amounts to the elucidation of the cross-relaxation networks in regions a and b (Figure 1) and correlating these with the known sequences of the DNA strands. This is demonstrated schematically in Figure 2.

Figure 2 shows a schematical 2-D NOE spectrum of a single DNA strand, consisting of three nucleotides in a right-handed helix conformation. Only the B, H1′, H2′, and H2″ resonances are shown, with their cross peaks, in one of the symmetrical triangles of the spectrum. The assignment procedure may start at any position in the chain. For simplicity let us start at the 5′ end with resonance B(1) (Figure 2). At the frequency $\omega_1 = \Omega_{B(1)}$ only intranucleotide cross peaks are found in region a [B–H1′(1,1)] and region b [B–H2′(1,1) and B–H2″(1,1)] as expected for a 5′-terminal residue (see Table I). A pair of cross peaks in region c [H1′–H2′(1,1) and H1′–H2″(1,1)] confirms the three deoxyribose resonance assignments. The position of the B(2) resonance of the 3′-neighboring nucleotide follows from cross peaks of the type B–H1′(2,1), B–H2′(2,1), or B–H2″(2,1). At this new frequency $\omega_1 = \Omega_{B(2)}$ also the intranucleotide cross peaks B–H1′(2,2), B–H2′(2,2), and

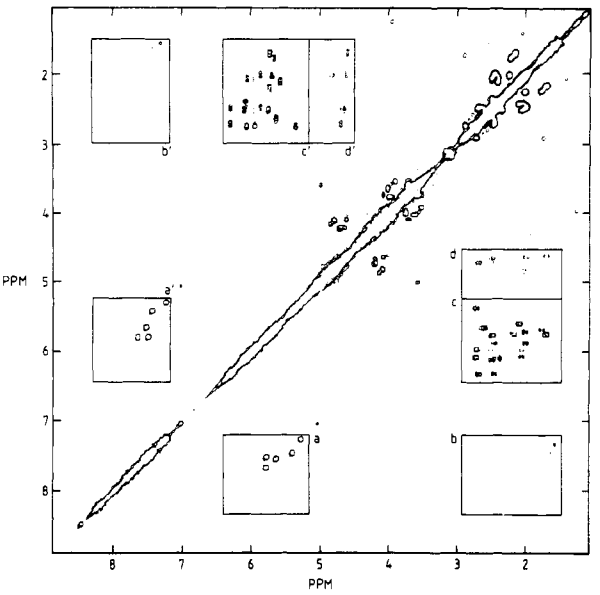

FIGURE 3: 500-MHz COSY spectrum of the 7 bp DNA duplex. A total of 64 scans was recorded for each FID. The boxed regions correspond to those in Figure 1.

B–H2″(2,2) are found. These new sugar resonances are again reflected by a pair of cross peaks H1′–H2′(2,2) and H1′–H2″(2,2) in region c. This completes the first step, which can be repeated until the resonances of the 3′-terminal nucleotide are located.

Figure 3 presents a COSY spectrum of the same DNA fragment. This spectrum can be used to establish the *J*-coupling patterns within each nucleotide. Thus, the COSY spectrum yields first-stage assignments (as to resonance type) of the cytosine H6 and H5 resonances, which give rise to the cross peaks in region a, and of the thymine H6 and 5-methyl resonances by their cross peaks in region b (Figure 3). By use of these first-stage assignments, the dipolar-coupling network can be correlated to the known base sequence, yielding the assignments of the adenine H8, guanine H8, cytosine H6 and H5, thymine H6 and 5-methyl, and the deoxyribose H1′ and H2′, H2″ resonances. Both COSY and 2-D NOE spectra can then be used to assign the remaining H3′, H4′, H5′, and H5″ resonances. In the oligonucleotides of the size we are studying, however, some of these assignments may be difficult to obtain by resonance overlap, especially in the H4′, H5′, H5″ region of the spectrum.

Application to a Duplex of d(TGAGCGG) and d-(CCGCTCA). The method was applied to an equimolar mixture of the two complementary heptanucleotides d-(TGAGCGG) and d(CCGCTCA), which form a double helix under the conditions employed.

The COSY spectrum of this duplex (Figure 3) yields the five CH6–CH5(*i*,*i*) (region a) and the two TH6–TCH$_3$(*i*,*i*) connectivities (region b).

Figure 4 shows enlarged the regions b and c and Figure 5 the regions a and c′ of the 2-D NOE spectrum. In region c (and its symmetrical counterpart c′) 14 pairs of cross peaks define the H1′–H2′(*i*,*i*) and H1′–H2″(*i*,*i*) connectivities. Each of these H1′, H2′, and H2″ resonances (except those of the 3′-terminal nucleotides G7 and A7) shows cross peaks in regions a and b with *two* B resonances,[3] establishing the connections B(*i*)–H1′, H2′, H2″(*i*)–B(*i* + 1). Together these steps define the cross-relaxation networks depicted in regions a and b (Figures 5 and 4). From the COSY spectrum (see above) we know which of the B resonances belong to cytosine or thymine residues, so that each network can be correlated uniquely to the base sequence of one of the two DNA strands.

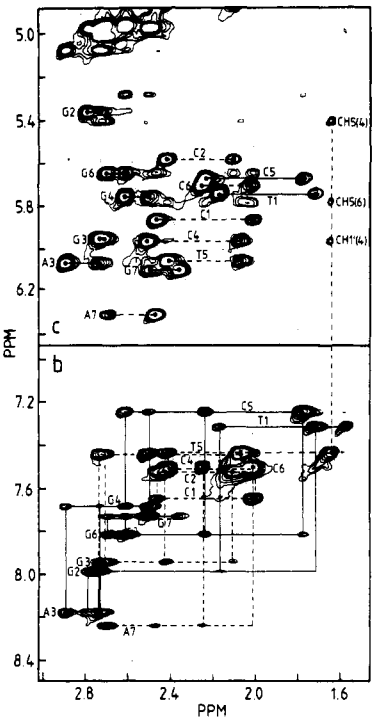

FIGURE 4: Regions b and c of the 2-D NOE spectrum of Figure 1. Drawn lines connect cross peaks involving resonances of the d-(TGAGCGG) strand and broken lines those of d(CCGCTCA). Intranucleotide contacts are indicated with a dot. Region c shows the H1′–H2′, H2″(*i*,*i*) and some contacts involving TCH$_3$(5); region b shows the B–H2′, H2″ and TH6–TCH$_3$ contacts.

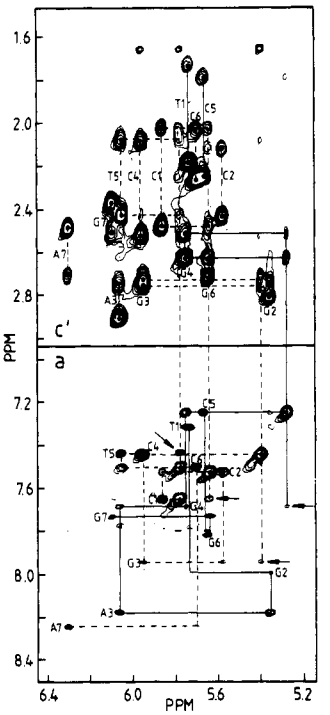

FIGURE 5: Regions a and c′ of the 2-D NOE spectrum of Figure 1 showing cross peaks of the type H2′, H2″–H1′(*i*,*i*) and H2′, H2″–CH5(*i*,*i* + 1) in region c′ and B–H1′ and B–CH5 cross peaks in region a. The internucleotide B–CH5(*i*,*i* + 1) contacts are indicated with an arrow. See legend to Figure 4 for further explanation.

[3] The TH6–GH2′(1,2) and the TH6–GH1′(1,2) cross peaks fall below the lowest contour level shown in Figures 4 and 5, respectively. They are more intense in a 2-D NOE spectrum recorded with a longer mixing time (τ_m = 0.2 s; Scheek et al., 1983).

Table II: Chemical Shifts of Assigned ^{1}H Resonances (in ppm, Relative to DSS) in the Duplex of d(TGAGCGG) and d(CCGCTCA)

	H8 or H6	CH5 or TCH_3	H1′	H2′	H2″	H3′	H4′	H5′, H5″[a]
T1	7.31	1.58	5.74	1.73	2.18	4.62	4.02	NA
G2	7.99		5.36	2.74	2.80	4.98	4.31	4.04, 3.95
A3	8.18		6.06	2.74	2.90	5.08	4.46	4.22, 4.14
G4	7.69		5.75	2.50	2.62	4.98	4.39	4.21, 4.20
C5	7.25	5.28	5.67	1.79	2.25	4.79	4.12	NA
G6	7.82		5.65	2.62	2.71	4.95	4.33	4.07, 3.98
G7	7.73		6.10	2.50	2.37	4.65	4.22	NA
C1	7.65	5.78	5.86	2.02	2.47	4.63	4.10	NA
C2	7.52	5.64	5.58	2.12	2.43	4.86	4.15	NA
G3	7.94		5.95	2.71	2.76	5.02	4.41	4.14, 4.06
C4	7.44	5.40	5.96	2.08	2.52	4.74	4.25	NA
T5	7.43	1.65	6.05	2.08	2.42	4.86	4.16	NA
C6	7.50	5.78	5.70	2.03	2.25	4.82	4.09	NA
A7	8.24		6.30	2.70	2.48	4.71	4.21	NA

[a] NA, not assigned.

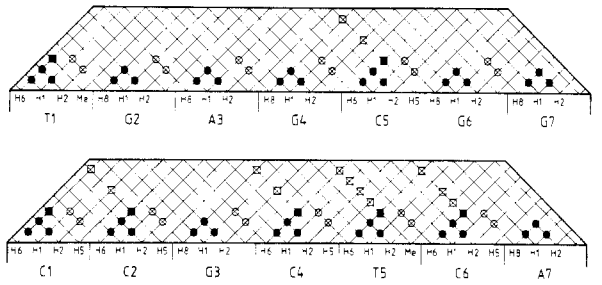

FIGURE 6: Summary of NOE cross peaks used for sequential assignments of the purine H8, pyrimidine H6, cytosine H5, thymine CH_3, and the deoxyribose H1′, H2′, and H2″ resonances. Not shown are the NOE contacts involving H3′, H4′, H5′, and H5″ resonances. Closed symbols denote the intranucleotide contacts and open symbols the internucleotide contacts. Cross peaks indicated with squares involve the CH5 or TCH_3 resonances of pyrimidine-containing nucleotides, and those with circles are found in both purine- and pyrimidine-containing nucleotides.

This leads to the assignments of the B, H1′, H2′, and H2″ resonances presented in Table II.

The remaining cross peaks in regions a, b, and c all involve CH5 or TCH_3 resonances. From the five CH6–CH5(i,i) and the two TH6–TCH_3(i,i) cross peaks, which are present both in the COSY and in the 2-D NOE spectrum (regions a and b, respectively), the CH5 and TCH_3 assignments follow directly. These resonances take part in alternative connections between B resonances via B–CH5(i,i + 1) and B–TCH_3(i,i + 1) contacts (see Table I). Thus, Figure 5 shows the four B–CH5(i,i + 1) contacts expected in region a, which define, together with the intranucleotide B–CH5 cross peaks, connections of the type B(i)–CH5(i + 1)–B(i + 1). The only B–TCH_3(i,i + 1) cross peak expected in region b [that between CH6(4) and TCH_3(5)] overlaps with the TH6–TCH_3(5,5) cross peak. Other internucleotide cross peaks involving CH5 and TCH_3 resonances are of the type H2′, H2″–CH5(i,i + 1) indicated in region c′ (Figure 5) and H2′, H2″–TCH_3(4,5). In addition some interesting long-range contacts between TCH_3(5) and CH5(4), CH5(6), and H1′(4) are visible in region c (Figure 4). Figure 6 summarizes all types of cross peaks that were identified in the 2-D NOE spectrum thus far.

Assignments of the H3′, H4′, H5′, and *H5″ Resonances.* Figure 7 presents enlarged the regions c and d of the 2-D NOE spectrum. In region d the 14 pairs of H3′–H2′, H2″(i,i) cross peaks can be identified. From the known H2′, H2″ assignments, those of the H3′ resonances follow directly. Alternatively, the H3′ assignments follow from H1′–H3′(i,i) cross peaks. Significantly stronger than these are 14 H1′ cross peaks (Figure 8, region e) between 4 and 4.5 ppm, which were identified as H1′–H4′(i,i) contacts and led directly to all H4′

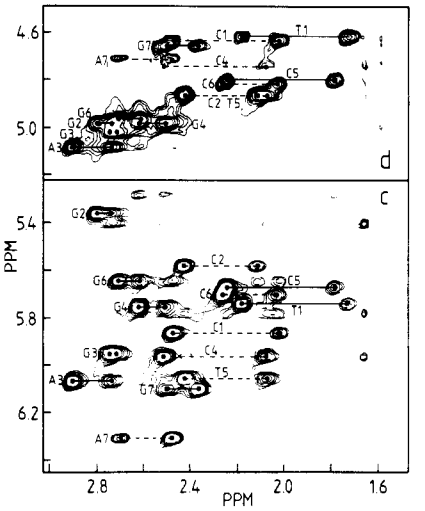

FIGURE 7: Regions c and d of the 2-D NOE spectrum of Figure 1 showing H1′–H2′, H2″(i,i) and H3′–H2′, H2″(i,i) cross peaks in regions c and d, respectively. See legend to Figure 4 for further explanation.

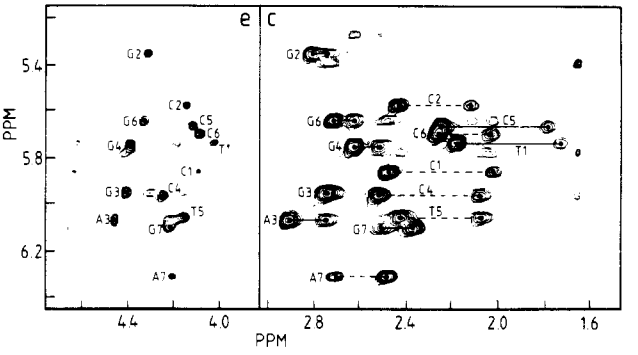

FIGURE 8: Regions e and c of the 2-D NOE spectrum of Figure 1 showing H1′–H4′(i,i) and H1′–H2′, H2″(i,i) cross peaks in regions e and c, respectively. See legend to Figure 4 for further explanation.

assignments. The H3′ and H4′ assignments thus found can be checked for consistency with the H3′–H4′(i,i) cross-peak region in the 2-D NOE or the COSY spectrum.

Pairwise assignment of some (purine) H5′ and H5″ resonances is possible via H3′–H5′, H5″(i,i) and H4′–H5′, H5″(i,i) cross peaks in the 2-D NOE spectrum. At this stage, however, overlap in the region of the H4′, H5′, and H5″ resonances hinders the complete assignment of all H5′, H5″ pairs. The resonance assignments found are collected in Table II.

Discrimination between H2′ and H2″ Resonances. Thus far the H2′ and H2″ resonances were assigned in a pairwise manner. They can be discriminated by a more quantitative

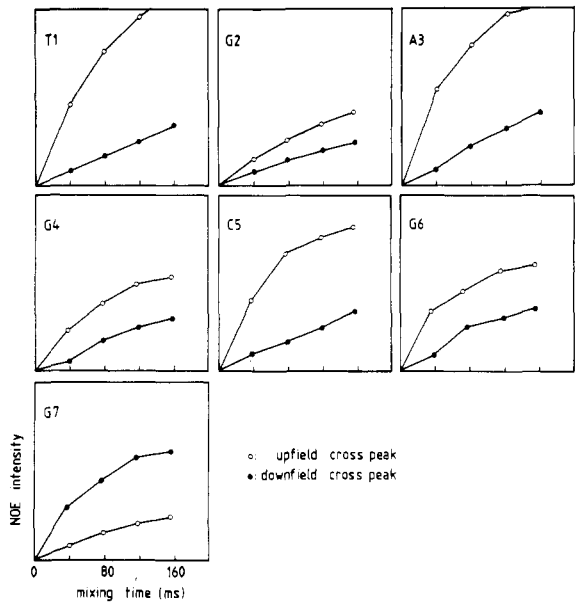

FIGURE 9: NOE buildup curves for the B–H2′(*i*,*i*) and B–H2″(*i*,*i*) contacts in the d(TGAGCGG) strand (see Figure 4b). Open circles denote the upfield cross peaks and closed circles the downfield cross peaks of the seven B–H2′, H2″(*i*,*i*) pairs. These curves are used to discriminate between H2′ and H2″ resonances.

analysis of cross-peak intensities. From Table I we conclude that in the anti conformation of the nucleotides the B–H2′(*i*,*i*) distance is significantly smaller than the B–H2″(*i*,*i*) distance. We compared the buildup rate of the corresponding cross peaks, as shown for the d(TGAGCGG) strand in Figure 9. Of each pair the more rapidly building-up cross peak, corresponding to the shorter proton–proton distance, was ascribed to the B–H2′(*i*,*i*) contact, leading to the assignments of the individual H2′ and H2″ resonances presented in Table II.

The B–H2′ distance in pyrimidines is slightly shorter (0.02 nm in regular B-DNA) than in purines. This explains the higher NOE buildup rate found for the B–H2′ cross peak in T1 and C5 compared with G4, G6, and G7 (Figure 9). In the case of G2 and A3 these buildup rates cannot be accurately determined because of overlap with other cross peaks (see Figure 4b). Thus, in a favorable case a 0.02-nm difference in proton–proton distance can be detected due to the r^{-6} dependence of the initial NOE buildup rate (Kumar et al., 1981).

Discussion

The advent of two-dimensional NMR techniques has made it possible to delineate complete networks of coupled nuclei in crowded ^{1}H NMR spectra. To a large extent this is due to the enormous resolution enhancement attainable in the two frequency domains. Sequential assignment procedures relate NMR coupling patterns to the known covalent structure of the molecule under investigation (Wüthrich et al., 1982). In small oligonucleotides the scalar-coupling network formed by the ribose ^{1}H and the ^{31}P resonances can be traced systematically by a combination of homo- and heteronuclear *J*-correlated spectroscopy, as demonstrated recently by Pardi et al. (1983). For larger oligonucleotides we propose here the use of 2-D NOE spectroscopy to analyze the dipolar-coupling network involving all nonexchangeable sugar and base protons (except adenine H2).

The success of 2-D NOE spectroscopy for this purpose has several causes. Unlike the case in *J*-correlated spectroscopy all multiplet components have the same phase in 2-D NOE spectra, so mutual cancelling due to poor resolution of the components does not occur. Furthermore, it is not necessary to perform an absolute-value calculation of the spectrum. As shown by States et al. (1982) it is possible to obtain pure absorption phase of both diagonal and cross peaks in all four quadrants of a 2-D NOE spectrum. It is our experience that the attainable signal-to-noise ratio in these spectra, given a certain resolution, is significantly better than in absolute-value spectra.

Some regularities concerning the chemical shifts of the ribose H2′ and H2″ resonances are apparent from Table II.

The H2″ protons generally resonate downfield from the H2′ protons, with the notable exception of those of the 3′-terminal nucleotides (G7 and A7). This suggests that the net negative charge on the 3′-phosphate groups, which is absent at the 3′-termini, has a profound effect on these chemical shifts. The directions of the C2′–H2′ and C2′–H2″ vectors in B-DNA are such that the polarizing effect of the negatively charged 3′-phosphate groups tends to shift the H2″ resonance to low and the H2′ resonance to high field. The absence of the 3′-terminal phosphates in our DNA fragment thus causes an upfield shift of the H2″ resonance, relative to H2′, explaining the reversal of the H2′ and H2″ resonance positions in A7 and G7.

The H2′ and H2″ of purines resonate at lower fields than those of pyrimidines, suggesting that the intranucleotide ring-current effect of the bases is a dominant factor in determining the chemical shift of these protons: the stronger ring current of purines causes more effective deshielding at the position of H2′ and H2″ than that of pyrimidines. However, no similar difference in chemical shift is apparent for purine H1′ vs. pyrimidine H1′. Probably this is due to the fact that at the position of the H1′ protons the C2 carbonyl bond anisotropy of pyrimidines compensates for the weaker deshielding effect of the pyrimidine ring current.

Similarly the C2 carbonyl bond anisotropy explains the larger difference in chemical shifts of H2′ and H2″ in pyrimidines when compared with those in purines: the deshielding effect of this bond is felt stronger at the position of H2″ than at H2′, which causes the relative downfield shift of the H2″ resonance in pyrimidine-containing nucleotides.

The present sequential assignment method is generally applicable to right-handed DNA duplexes (not only B-DNA) of intermediate size. We have recently applied the method successfully to a 14-bp *lac* operator fragment (to be published). Assignments were obtained for all 28 nucleotides except for some H4′, H5′, and H5″ protons.

Further work will be directed to obtaining more quantitative information about proton–proton distances from 2-D NOE spectroscopy in order to determine the solution structure of DNA duplexes.[4]

Acknowledgments

We thank P. A. W. van Dael, Dr. C. Haasnoot, and K. Dijkstra for their expert technical assistance and stimulating discussions.

Registry No. d(TGAGCGG)·d(CCGCTCA), 88496-04-2.

References

Arnott, S., & Hukins, D. W. L. (1972) *Biochem. Biophys. Res. Commun. 47*, 1504–1509.

Aue, W. P., Bartholdi, E., & Ernst, R. R. (1976) *J. Chem. Phys. 64*, 2229–2246.

[4] After preparation of this paper Dr. B. R. Reid (University of Washington, Seattle, WA) informed us that he had developed a very similar assignment procedure and applied it to a self-complementary dodecamer.

Bell, R. A., Alkema, D., Coddington, J. M., Dader, P. A., Hughes, D. W., & Neilson, T. (1983) *Nucleic Acids Res. 11*, 1143–1149.
De Rooij, J. F. M., Wille-Hazeleger, G., Van Deursen, P. H., Serdijn, J., & Van Boom, J. H. (1979) *Recl. Trav. Chim. Pays-Bas 98*, 537–548.
Feigon, J., Wright, J. M., Leupin, W., Denny, W. A., & Kearns, D. R. (1982) *J. Am. Chem. Soc. 104*, 5540–5541.
Kumar, A., Wagner, G., Ernst, R. R., & Wüthrich, K. (1981) *J. Am. Chem. Soc. 103*, 3654–3658.
Macura, S., & Ernst, R. R. (1980) *Mol. Phys. 41*, 95–117.
Pardi, A., Walker, R., Rapoport, H., Wider, G., & Wüthrich, K. (1983) *J. Am. Chem. Soc. 105*, 1652–1653.
Patel, D. J., Kozlowski, S. A., Marky, L. A., Broka, C., Rice, J. A., Hakura, K., & Breslauer, K. J. (1982) *Biochemistry 21*, 428–436.
Redfield, A. G., Roy, S., Sanches, V., Tropp, J., & Figueroa, N. (1981) in *2nd Biomolecular Stereodynamics Conference* (Sarma, R., Ed.) pp 195–208, Academic Press, New York.
Scheek, R. M., Russo, N., Boelens, R., & Kaptein, R. (1983) *J. Am. Chem. Soc. 105*, 2914–2916.
States, D. J., Haberkorn, R. A., & Ruben, D. J. (1982) *J. Magn. Reson. 48*, 286–292.
van Boom, J. H., Burgers, P. H. J., & Van Deursen, P. H. (1976) *J. Mol. Biol. 155*, 311–319.
Wüthrich, K., Wider, G., Wagner, G., & Braun, W. (1982) *J. Mol. Biol. 155*, 311–319.
Zuiderweg, E. R. P., Scheek, R. M., Veeneman, G., van Boom, J. H., Kaptein, R., Rüterjans, H., & Beyreuther, K. (1981) *Nucleic Acids Res. 9*, 5175–5184.
Zuiderweg, E. R. P., Kaptein, R., & Wüthrich, K. (1983) *Proc. Natl. Acad. Sci. U.S.A. 80*, 5837–5841.

Magnesium Binding and Conformational Change of DNA in Chromatin†

Kazutada Watanabe‡ and Koujiro Iso*

ABSTRACT: The structure of chromatin in the presence of Mg^{2+} ions was examined by circular dichroism and equilibrium dialysis. (1) Circular dichroism (CD) shows that above 260 nm the intensity of the spectrum of DNA in nucleoproteins decreases as the Mg^{2+} concentration increases. This change is an intrinsic characteristic of DNA since it is also observed in protein-free DNA and has been attributed to a change in the winding angle of base pairs around the DNA axis. Some structural elements of the DNA in the nucleosome core, therefore, are as movable as those of protein-free DNA. (2) The basic organization of H1-depleted chromatin, 146 base pairs (bp) of DNA wound around core histones and a residual 49 bp in the linker region in the repeating unit, is maintained both in the presence and in the absence of Mg^{2+} ions, as shown by the fact that the CD spectrum of H1-depleted chromatin has the same type of linear combination between the spectrum of protein-free DNA and that of the nucleosome core in 0.2 mM $MgCl_2$–10 mM triethanolamine (pH 7.8) as it has in 1 mM ethylenediaminetetraacetic acid–10 mM tris(hydroxymethyl)aminomethane (pH 7.8). (3) The ellipticity of chromatin shows a smaller decrease relative to the other nucleoproteins and protein-free DNA upon the addition of Mg^{2+} ions. Therefore, some structural elements of chromatin are apparently somewhat protected against the conformational change induced by these ions. The spectrum of chromatin becomes almost indistinguishable from that of H1-depleted chromatin in 0.2 mM $MgCl_2$. (4) The number of phosphate groups which do not experience interference with Mg^{2+} ion binding by core histones is calculated to be at least 2 per 10 phosphate groups in the nucleosome core. Therefore, it is suggested that these groups are located on the outer surface of the nucleosome core DNA and are easily attacked by DNase I. (5) Chromatin binds less Mg^{2+} ions than H1-depleted chromatin. This may be due to the effect of H1 itself or the formation of higher order structure of chromatin.

The magnesium ion is widely distributed in biological systems and plays an important role in many enzymatic activities, especially reactions involved in replication, transcription, and translation. Ribosomes, transfer RNA, and many enzymes involved in these processes lose their biological activity in the absence of this ion. Furthermore, it is known that the magnesium ion maintains the tertiary structure of transfer RNA (Lindahl et al., 1966; Lynch & Schimmel, 1974a; Quigley et al., 1978) and the folding of ribosomal particles (Weiss & Morris, 1973a,b; King et al., 1981). The stability of double-helical DNA against thermal denaturation is also greatly enhanced by magnesium ions. Thus, a great deal of data on magnesium binding to DNA, transfer RNA, and ribosomes has been reported (Edelman et al., 1960; Choi & Carr, 1967; Sander & T'so, 1971; Danchin, 1972; Clement et al., 1973; Lynch & Schimmel, 1974a,b; Reuben & Gabbay, 1975).

In the formation of a higher order structure and condensation of chromatin, the requirement and effectiveness of magnesium ions has already been reported by many researchers (Leake et al., 1972; Billett & Barry, 1974; Finch & Klug, 1976; Kiryanov et al., 1976; Sperling & Klug, 1977; Thoma et al., 1979; Langmore & Schutt, 1980; McGhee et al., 1980). It is generally accepted that histone H1 is responsible for the formation of this structural organization of chromatin in the presence of magnesium ions. Histone H1 plays a significant role in the condensation of chromatin (Bradbury et al., 1973; Billett & Barry, 1974; Osipova et al., 1980) and is necessary for the formation of the 300-Å-thick fibers of chromatin (Thoma et al., 1979; McGhee et al., 1980). The effect of magnesium ions on the reversible swelling and contraction of chromatin and the nuclei has been examined in relation to its transcriptional activity (Leake et al., 1972),

† From the Department of Chemistry, College of Arts and Sciences, University of Tokyo at Komaba, Meguro-ku, Tokyo 153, Japan. *Received May 24, 1983; revised manuscript received November 7, 1983.*
‡ Present address: Oncology Unit, Faculty of Medicine, University of Calgary, Calgary, Alberta, Canada T2N 4N1.

0006-2960/84/0423-1376$01.50/0